

## Three Methods for Mitigating Airwaves in Shallow Water Marine CSEM Data

Jiuping Chen\*, and David Alumbaugh, Schlumberger, 1301 S.46<sup>th</sup> Street # 300, Richmond, CA94804, USA

### Summary

Over the past several years, Marine Controlled-Source EM (MCSEM) techniques have been successfully applied in deep water (water depth >1 km) for oil/gas exploration. In contrast, application of this technology in shallow water, although available, is challenged due to ‘airwaves’ that mask the signal from the target reservoir at depth. Based upon ‘lateral wave’ theory, we propose three airwave-mitigation approaches to reduce the effects of these arrivals on MCSEM data. By comparing the detectability of a target in deep water versus shallow water for models including bathymetry, we show that the airwave effects in a shallow water environment can be reduced leading to a greater reservoir detectability.

### Introduction

Marine Controlled-Source ElectroMagnetics (MCSEM) has been applied as a useful tool to derisk oil/gas exploration in the ocean environment. This method uses a high-powered horizontal electric dipole (HED) to transmit a low-frequency (0.01 – 10 Hz) EM signal through seawater column and seafloor. The source is typically towed just above an array of multicomponent EM receivers that are deployed on seafloor to record the generated EM responses. By analyzing these EM responses, the bulk electrical resistivity of seafloor sediments can be estimated both as a function of lateral position and more importantly, depth. Because oil is relatively resistive compared to conductive sediments, the resulting resistivity analysis can be used to determine the probability that a given region of the subsurface contains hydrocarbon [Young and Cox, 1981; Chave and Cox, 1982; Eidesmo et al., 2002; Srnka et al., 2006].

The depth of the seawater column has strong influence on measured EM signals. Because of this, early applications of MCSEM for hydrocarbon exploration concentrated on targets in deep water scenarios, where the water depth is generally greater than 1 km [Andreis and MacGregor, 2008]. Conventional transmitters are towed deep to maximize EM coupling between sources, receivers and reservoir targets, as well as to mitigate the so-called “airwave” effects [Constable, 2003; Lu et al., 2005; LØseth et al., 2008]. The airwave effects are notorious in shallow water, where the useful signals from the reservoir targets might be totally masked by the airwaves, which generally are thought to contain little information about the subsurface.

Because the airwave masks the deeper reservoir signal, much effort has been devoted to this problem. Several techniques have been published for dealing with frequency-domain (FD) EM data; these include subtraction of a background model response from a total field [Lu et al., 2005], up- and down-ward separation of the

measured fields [Amundsen, 2003], measurement of vertical electric fields [Constable, 2003], combining spatial derivatives of the measured electric and magnetic fields [MacGregor and Sinha, 2004], direct computation of the airwaves [Weidelt, 2007; Nordskog and Amundsen, 2007], using crossed-dipole sources [LØseth and Amundsen, 2007], and using reciprocity/decomposition of EM fields [van den Burg et al., 2008]. In the time-domain (TD), the airwaves are considered to be separable in the early time data [Ziolkowski and Wright, 2007], although their effects still might prevail and interfere with other components in the mid time range [Weiss, 2007].

Based upon the understanding of the airwave as a ‘lateral wave’ [Clough, 1976; Bannister, 1984; King et al., 1992], we propose three new airwave-mitigation methods. These three methods are referred to as the (1) EM ‘lateral-bucking’, (2) the frequency derivative (dE/dFreq), and (3) MT impedance stripping approaches. In this paper, we analyze the usefulness of these approaches by applying them to shallow water FD MCSEM data. The analysis is provided by comparing deep water, shallow water, and airwave-mitigated shallow water responses, with and without realistic bathymetry.

### Three airwave-mitigation approaches

Bannister’s paper (1984) derives explicit expressions for the EM radial electric field produced by a horizontal electric dipole (HED) source in a dual-halfspace model in which the electromagnetic fields can be broken into three components (Figure 1): a direct component (D), a modified image component (I), and lateral wave (L). These three components can be distinguished from their travel paths, which are manifested analytically as shown in Eq. (1)

$$\begin{aligned}
 E_{\rho}(\rho, z, \phi) &= D + I + L \\
 &= \frac{p \cos \phi}{2\pi\sigma\rho^3} \left\{ [(1+k\rho) - (3+3k\rho+k^2\rho^2) \frac{(z-h)^2}{2\rho^2}] e^{-kR_0} \right. \quad (D) \\
 &\quad - [(3+3k\rho+k^2\rho^2) \frac{(z+h)^2}{2\rho^2}] e^{-kR_1} \quad (I) \\
 &\quad \left. + [(1+k_0\rho+k_0^2\rho^2 F)] e^{-k_0\rho} e^{-k(z+h)} \right\} \quad (L)
 \end{aligned}
 \tag{1}$$

where  $p$  is the dipole moment for the HED,  $R_0$  is the distance between the receiver and the HED,  $R_1$  is the distance between the receiver and the image source, and  $k$  is the wavenumber in the water, and  $F$  is the Sommerfeld surface-wave attenuation function, which can be approximated as  $F \cong 1.0$ .

The first term in the bracket of Eq. (1) is the direct field, which contains  $e^{-kR_0}$ . The second term is the reflected or modified

## Mitigation of Airwaves in Shallow Water

image field, which is expressed with the exponential term  $e^{-kR_1}$ . As shown in Fig. 1,  $R_1$  is the distance between the image source location (in the air) and Rx. The last term is most interesting, because it has an upward-path ( $e^{-kh}$ ), a path traveling along the interface of the air and water ( $e^{-k_0\rho}$ ), and downward-path ( $e^{-kz}$ ). This is the so-called ‘‘lateral wave’’ [Clough, 1976; Bannister, 1984; King et al., 1992].

For the upward-, and downward-segments, we can see that the field is traveling in water with a wavenumber  $k$  in the exponential terms  $e^{-kh}$  and  $e^{-kz}$ . But the segment traveling along the interface propagates with a wavenumber equivalent to that of air. Since  $|k_0|$  in the air is much smaller than  $|k|$  in water, the attenuation for the wave traveling along the interface is negligible, and thus the only attenuation for the lateral wave occurs in the upward- and downward-segments, which are directly related to Tx and Rx depth. We believe that this lateral wave describes the physics of the so-called ‘‘airwave’’ in a two-halfspace model. In addition, for more realistic 1D, 2D and 3D where the airwave is coupled to the sub-seafloor, empirical evidence indicates that expression (1) provides a good approximation for the airwave at least in terms of its spatial behavior.

In deep water, the sum of  $h$  and  $z$  is essentially two times the water depth. Therefore the interactions among the direct, image and airwave fields are manifested in the relationship of  $\rho$  and  $h+z$ . In near offsets, i.e.,  $\rho \ll h+z$ , the direct and image fields will be dominant in measurements, and the airwave part can be ignored. In large offsets, for example, when  $\rho \gg h+z$ , the direct and image fields will be attenuated heavily, and the remaining field will be the airwave. This explains why the airwave becomes dominant at far offsets. In between these two extremes, all three components are present with none dominant.

In contrast, for shallow water surveys, both the Tx and Rx are close to the air/water interface;  $h$  and  $z$  must be much smaller than the horizontal distance  $\rho$ . Therefore, when the horizontal distance  $\rho$  is large, we expect to see that the airwave dominates the total field, making it difficult to infer resistivity information from measurements. However, we can make use of certain characteristics of Eq.(1) to develop methods to mitigate these effects.

### Approach 1: EM ‘Lateral-bucking’

For a given tow line where the receiver depth ‘ $z$ ’ remains constant, we see from Eq.(1) that the airwave depends only on the horizontal distance between the source and receiver,  $\rho$ , and the depth of the transmitter,  $h$ . Thus if we have fairly accurate

estimates of  $\rho$  and  $h$ , we can cancel, or ‘buck out’ the airwave by combining multiple measurements. Here we use two measurements,  $E_1$  and  $E_2$  at the same Rx but with two Tx positions, using the expression

$$E_{12}^B = E_1 \left[ e^{-k(h_2-h_1)} \left( \frac{\rho_1}{\rho_2} \right)^3 \right] - E_2 \quad (2)$$

where  $\rho_1$  and  $h_1$  represent positions of the first Tx relative to the receiver, and  $\rho_2$  and  $h_2$  are the second Tx position. The usefulness of this approach relies on the reservoir response having a different geometrical fall-off versus source-receiver separation compared to the airwave which is generally the case. The horizontal distance between two transmitters used for removing the effect of the airwave is referred to as ‘bucking’ distance. Similarly we can apply this idea to two measurements associated with two Rxs but with the same Tx position.

### Approach 2: $dE/dFreq$

Taking the derivative of each part in Eq.(1) with respect to angular frequency, we find

$$\frac{\partial E_\rho}{\partial \omega} = \alpha_D \cdot D + \alpha_I \cdot I + \alpha_L \cdot L \quad (3)$$

where the three coefficients corresponding to  $D$ ,  $I$ , and  $L$  are

$$\alpha_D = \alpha_I \approx -\frac{1+i}{2\omega} \cdot \frac{\rho}{\delta} \quad (4)$$

and

$$\alpha_L = -\frac{1+i}{2\omega} \cdot \frac{z+h}{\delta} \quad (5)$$

where  $\delta$  is the skin depth in water. Equations 4 and 5 imply that compared with the original electric field, the derivatives for the  $D$  and  $I$  parts are enhanced as they depend mainly upon  $\rho$ , while the airwave, which is proportional to the water depth is increasingly suppressed as the water becomes shallower.

### Approach 3: MT impedance stripping

At larger offsets, the lateral wave component of the horizontal electric field ( $E_x^L$ ) can be approximated as

$$E_x^L \approx \frac{P}{2\pi\sigma\rho^3} e^{-k(z+h)} \quad (6)$$

which resembles a vertically propagating/diffusing plane-wave. Note this is the same phenomena employed in the far field for the CSAMT method. Under this assumption, the horizontal electric and magnetic fields in a one-dimensional earth satisfy

$$E_x^L = Z_{xy} \cdot H_y^L \quad (7)$$

where  $H_y^L$  is the horizontal y-component of lateral-wave-generated magnetic field, and  $Z_{xy}$  is the *plane-wave* or *MT*

## Mitigation of Airwaves in Shallow Water

impedance of the medium. Because these fields are entirely horizontal, there is no sensitivity to the reservoir.

The impedance  $Z_{xy}$  can be obtained by making measurements of naturally occurring plane-wave fields via a marine MT survey. These data are measured during a MCSEM survey when the source is distant from the receivers such that the CSEM fields are smaller in amplitude than the naturally occurring fields, or during the source current is off. Subtracting this term from the measured electric field in the MCSEM will define a new quantity, which is called as the 'scattered' electric field ( $E_x^{scat}$ )

$$E_x^{scat} = E_x^{CSEM} - Z_{xy} \cdot H_y^{CSEM} \quad (8)$$

Note that  $Z_{xy} H_y^{CSEM}$  essentially estimates the plane-wave component of the electric field which is insensitive to the reservoir. Also both CSEM and MT should have an overlapped frequency range.

### Applications to shallow water

To provide an understanding to the effects of the airwave, as well as test the three mitigation methods, we have designed four different 2D target scenarios as shown in Fig. 2: a deep water (water depth 3 km) model with a flat seafloor (DF), a shallow water model (water depth 0.1 km) with a flat seafloor (SF), a deep water model with bathymetry (DB), and a shallow water model with bathymetry (SB). In all the four scenarios, receivers are assumed to be deployed at the seafloor, and transmitters are kept 50 m above the seafloor. The reservoir target is a resistive slab (20  $\Omega$ -m) with a length of 9 km, and a thickness of 50 m, about 1.6 km below the seafloor, and embedded in a 4-layered sea bed. Although the depth of the slab is different relative to the sea surface in the deep and shallow water, its location below the seafloor remains constant. The variation of the bathymetry is roughly 1 km over a 30 km long profile. The corresponding background model without the slab target is used for calculating the detectability (or normalized response) in each scenario.

In the computation of 2.5D CSEM model responses, sixty-eight inline electric-dipoles, separated by 0.5 km, and thirty-one receivers with a spacing of 1 km, were employed using the 2.5D forward algorithm described in Abubakar et al. [2008]. Both inline  $E_x$  and crossline  $H_y$  components were simulated for the background and target models. We tested the methods for a variety of frequencies ranging from 0.0625 Hz to 1.25 Hz. Here only 0.25 Hz data will be presented due to space limitations. For the MT stripping approach, 2D MT impedance (TM mode) data were computed using a finite difference algorithm. The detectability is calculated as the ratio between the response with the target and the background model without the target, and plotted and contoured as a function of transmitter and receiver position. Note that a noise floor of  $1.0 \times 10^{-15}$  V/m/(Am) for the electric field was assumed, and any computed field less than this

floor was set to this value. By doing this, the computed normalized response will guarantee that any anomaly, especially at larger offsets, that falls below standard noise levels, will be excluded.

In deep water (model DF and DB on the left two panels), both with and without bathymetry, we have up to a factor of 2 difference in signal between the target and background models, i.e., we have a maximum of 100% increase in the target response, compared to the background (see Figure 3). On the contrary, in shallow waters (model SF and SB on the right two panels), the detectabilities are significantly smaller, suggesting that the reservoir will be difficult to detect in these scenarios. This plot confirms the perception that the current MCSEM method is best applied in deep waters.

When we apply the three airwave-mitigating approaches to the shallow water data (with and without bathymetry), the detectability increases significantly. As shown in Figure 4, all the three approaches significantly enhance the detectability, making the reservoir response stand out almost as well as if the data were acquired in deep water. This is especially true for the MT stripping approach, which seems to best reproduce the deepwater response. However, because we are combing the data in different ways to remove the airwave component, the various approaches exhibit different features. For example, using a bucking distance of 2 km, the lateral-bucking results resemble the MT stripping in the flat model, because both approaches are designed to completely remove the airwave from the measured data. On the other hand, the  $dEx/dFreq$  is aimed to reduce the airwave part of the relative to the other components. The  $dEx/dFreq$  data has a relatively larger anomaly but is more focused in space and is accompanied by side lobes where the detectability less than 1. Further discrepancies appear in the bathymetric models (three lower panels). The lateral-bucking result shows characteristics that suggest that the bathymetry affects this method more than in the other two approaches. As a whole, these results demonstrate the possibility of these types of airwave mitigation approaches on MCSEM data collected in shallow water to enhance subsurface target responses.

### Conclusions

We present a detectability analysis where three different airwave-mitigation approaches are applied to synthetic MCSEM data generated from shallow water models that can include bathymetry. When analyzed without processing, the shallow-water data show much less detectability than the corresponding deep-water data. However, with the help of the three airwave-correction methods, we gain back at least some of the detectability that is lost due to the airwave masking effect. To a certain degree, the mitigated data appear to be equivalent to the data acquired in a deep water. In addition, these three approaches can be applied to data acquired by standard MCSEM technology without change to acquisition methods or layouts.

## Mitigation of Airwaves in Shallow Water

However, the usefulness of these methods will be dependent on characteristics of the noise, and reservoir signal levels relative to the airwave. Further research to examine detectability via inversion results will make them practically more useful.

### Acknowledgement

We are grateful to WesternGeco/Schlumberger for permission to publish this work.

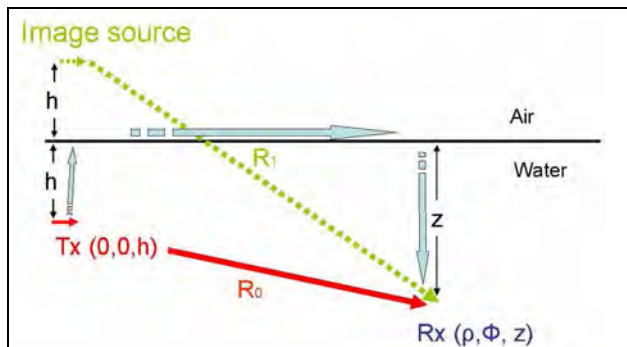


Figure 1: A schematic of EM fields due to a horizontal electric dipole (HED) source in a two uniform half-space model. The travel paths of the three components: direct (D), modified image (I), and lateral wave (L) are denoted in red, yellow green and light blue arrows, respectively.

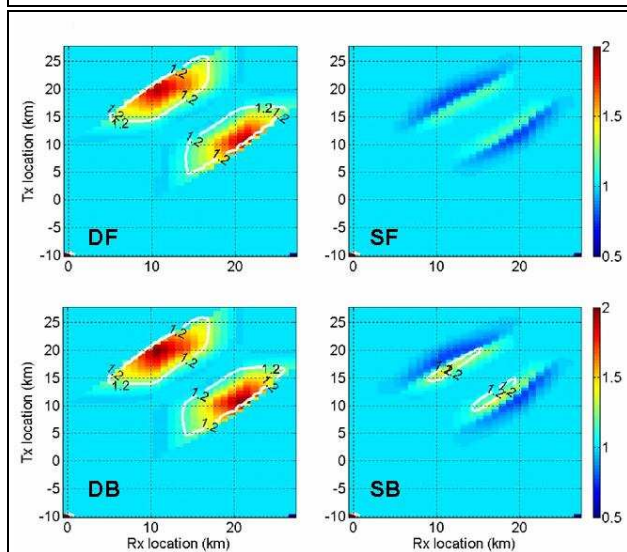


Figure 3: Detectabilities (or normalized field) of the 'raw' inline Ex fields to the slab target in the 4 scenarios shown in Figure 2. The horizontal axis represents Rx locations and the vertical Tx locations, i.e., each data point is associated with a specific pair of Tx and Rx location.

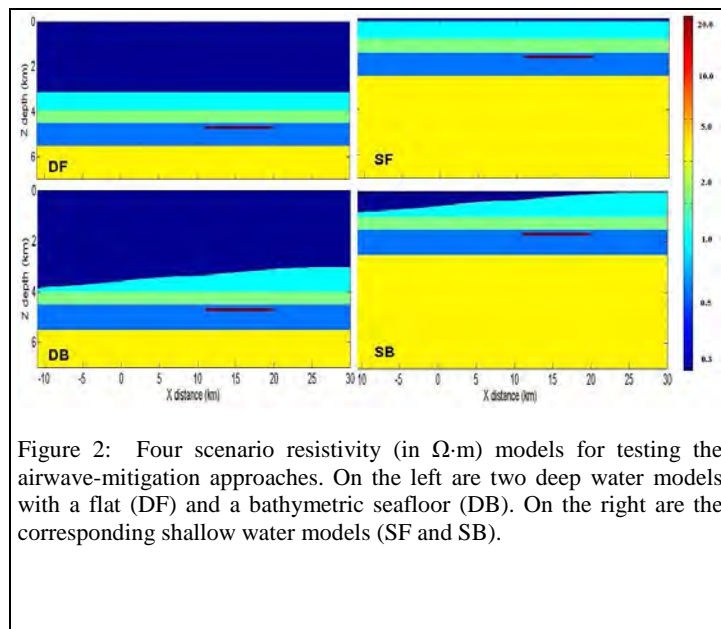


Figure 2: Four scenario resistivity (in  $\Omega\text{-m}$ ) models for testing the airwave-mitigation approaches. On the left are two deep water models with a flat (DF) and a bathymetric seafloor (DB). On the right are the corresponding shallow water models (SF and SB).

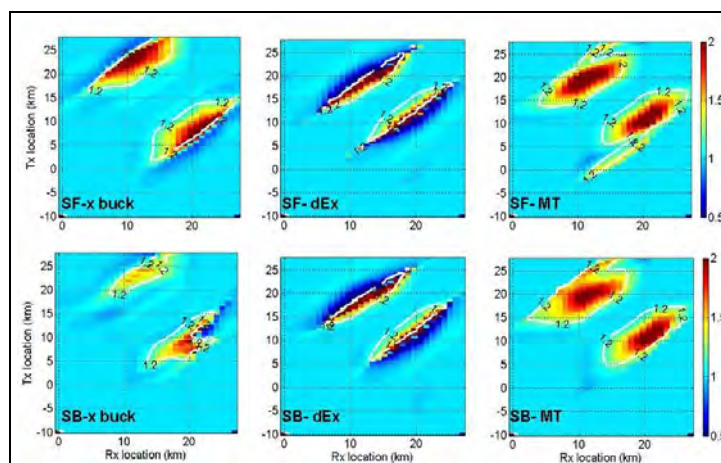


Figure 4: Detectabilities of the airwave-mitigated Ex fields for the two shallow water models (model SF on top and SB on the bottom). 'Lateral-bucking' is on the left two panels; dEx/dFreq is in the middle, and MT stripping on the right.

## EDITED REFERENCES

Note: This reference list is a copy-edited version of the reference list submitted by the author. Reference lists for the 2009 SEG Technical Program Expanded Abstracts have been copy edited so that references provided with the online metadata for each paper will achieve a high degree of linking to cited sources that appear on the Web.

## REFERENCES

- Abubakar, A., T. Habashy, V. L. Druskin, L. Knizhnerman, and D. Alumbaugh, 2008, 2.5D forward and inverse modeling for interpreting low-frequency electromagnetic measurements: *Geophysics*, **73**, no. 4, F165–177.
- Amundsen, L., 2003, System and method for electromagnetic wavefield resolution: Technical Report PCT Publication, WO200100467, Patent Office.
- Andrés, D., and L. MacGregor, 2008, Controlled-source electromagnetic sounding in shallow water: Principles and applications: *Geophysics*, **73**, no. 1, F21–F32.
- Bannister, P., 1984, New simplified formulas for ELF subsurface-to-subsurface propagation: *IEEE Journal of Oceanic Engineering*, **OE-9**, 154–163.
- Chave, A., and C. S. Cox., 1982, Controlled electromagnetic sources for measuring electrical conductivity beneath the oceans: *Journal of Geophysical Research*, **87**, 5327–5338.
- Clough, J. W., 1976, Electromagnetic lateral waves observed by earth-sounding radars: *Geophysics*, **41**, 1126–1132.
- Constable, S. C., 2003, Method and system for seafloor geological survey using vertical electric field measurement: Technical Report PCT Publication, WO03104844 A1, Patent Office.
- Eidesmo, T., S. Ellingsrud, L. W. MacGregory, S. Constable, M. C. Sinha, S. Johansen, F. N. Kong, and H. Westerdahl, 2002, Sea Bed Logging (SBL), a new method for remote and direct identification of hydrocarbon filled layers in deepwater areas: *First Break*, **20**, 144–152.
- King, R. W. P., M. Owens, and T. T. Wu, 1992, Lateral electromagnetic waves: Theory and applications to communications, geophysical exploration, and remote sensing: Springer-Verlag.
- Løseth, L. O., and L. Amundsen, 2007, Removal of air-response by weighting inline and broadside CSEM/SBL data: 77th Annual International Meeting, SEG, Expanded Abstract, 529–533.
- Løseth, L. O., H. M. Pedersen, T. Schaug-Pettersen, S. Ellingsrud, and T. Eidesmo, 2008, A scaled experiment for the verification of the seabed logging method: *Journal of Applied Geophysics*, **64**, 47–55.
- Lu, X., L. J. Srnka, and J. J. Carazzone, 2005, Method for removing air wave effect from offshore frequency domain controlled-source electromagnetic sounding data: Technical Report PCT Publication, WO2005010560, Patent Office.
- MacGregor, L., and M. Sinha, 2004, Electromagnetic surveying for hydrocarbon reservoirs: Technical Report PCT Publication: WO2004109338, Patent Office.
- Nordskog, J. I., and L. Amundsen, 2007, Asymptotic airwave modeling for marine controlled-source electromagnetic surveying: *Geophysics*, **72**, no. 6, F249–255.
- Srnka, L., J. Carazzone, J., and M. Ephron, 2006, Remote reservoir resistivity mapping: *The Leading Edge*, **25**, 972–975.
- van den Berg, P. M., T. M. Habashy, and A. Abubakar, 2008, Removing sea-surface-related electromagnetic fields in performing an electromagnetic survey: US 2008/0103700 A1.
- Weidelt, P., 2007, Guided waves in marine CSEM: *Geophysical Journal International*, **171**, 153–176.
- Weiss, C.J., 2007, The fallacy of the “shallow-water problem” in marine CSEM exploration: *Geophysics*, **72**, no. 6, A93–A97.
- Young, P., and C. Cox, 1981, Electromagnetic active source sounding near the east Pacific rise: *Geophysical Research Letters*, **8**, 1043–1046.
- Ziolkowski, A., and D. Wright, 2007, Removal of the air wave in shallow marine transient EM data: 77th Annual International Meeting, SEG, Expanded Abstract, 534–538.